EUROfusion

WPHCD-PR(17) 17595

Ia Morgal et al.

Characterization of a rf inductive plasma driver on the Cybele ion source for the future photo-neutralization based NBI system

Preprint of Paper to be submitted for publication in
Nuclear Fusion

This work has been carried out within the framework of the EUROfusion Consortium and has received funding from the Euratom research and training programme 2014-2018 under grant agreement No 633053. The views and opinions expressed herein do not necessarily reflect those of the European Commission.

Characterization of a rf inductive plasma driver on the Cybele ion source for the future photo-neutralization based NBI system

Ia. Morgal[1] , G.Cartry[1], C.Grand[2], A.Simonin[2].
[1]*Aix-Marseille University, CNRS, PIIM, UMR 7345, F-13013 Marseille, France.*
[2]*CEA-Cadarache, IRFM, F-13108 St. Paul-les-Durance, France.*

Corresponding author: iaroslav.morgal@cea.fr

Abstract. To provide heating and current drive on a future fusion reactor (DEMO), the relevant NBI systems will have to provide a high neutral power, i.e. between 50 and 150 MW of D° beam at 1MeV, including high wall-plug efficiency (η > 60%). For this purpose, a new injector concept, called Siphore, is under investigation at CEA. Siphore is based on the photodetachment of the energetic negative ions (the 1MeV D^-) by high power photon beams provided by several Fabry-Perot cavities implemented along the 1MeV D^- beam. To maximize the overlap of the D^- beam by the photon beams, the beamline is designed to be tall and narrow to provide thin negative ion beam sheets. The paper describes the present R&D at CEA which addresses the development of a RF ion source (called Cybele source) and accelerator dedicated to the Siphore topology. The Cybele source concept is based on a magnetized plasma column supplied by RF plasma generators implanted at the source extremities. The experimental results of Cybele equipped with a 1 MHz ICP-driver are described. The plasma parameters such as temperature, density are measured by the use of Langmuir probes. The paper highlights the low capability of the RF ICP driver to provide a dense and uniform plasma along the source column essential to attain the relevant negative ion density (J_D-~250 A/m^2) along the accelerator surface.

INTRODUCTION

The next generation of Neutral Beam Injection (NBI) systems, based on the acceleration of intense deuterium Negative (D^-) Ion beams dedicated to the DEMO reactor [1,2], is under investigation in CEA-IRFM in collaboration with universities in France and Switzerland. To this aim, a new concept of the neutral beam injection system [3] based on blade-like shaped beam is considered as a possible solution to provide high power neutral beams with high efficiency. Blade-like beams are essential for advanced neutralization concepts, like the photoneutralization of the energetic negative ions. If feasible, photoneutralization would be the ideal solution for the conversion of the energetic D^- to powerful neutral beams (D°) because it offers in the same time a complete suppression of the gas injection in the neutralizer (reduction of the D^- losses by stripping) , with a potentially high neutralization rate (> 90%). A blade-like topology is required for maximizing the overlap between the photon beams with the energetic ions beam (see Fig.1).

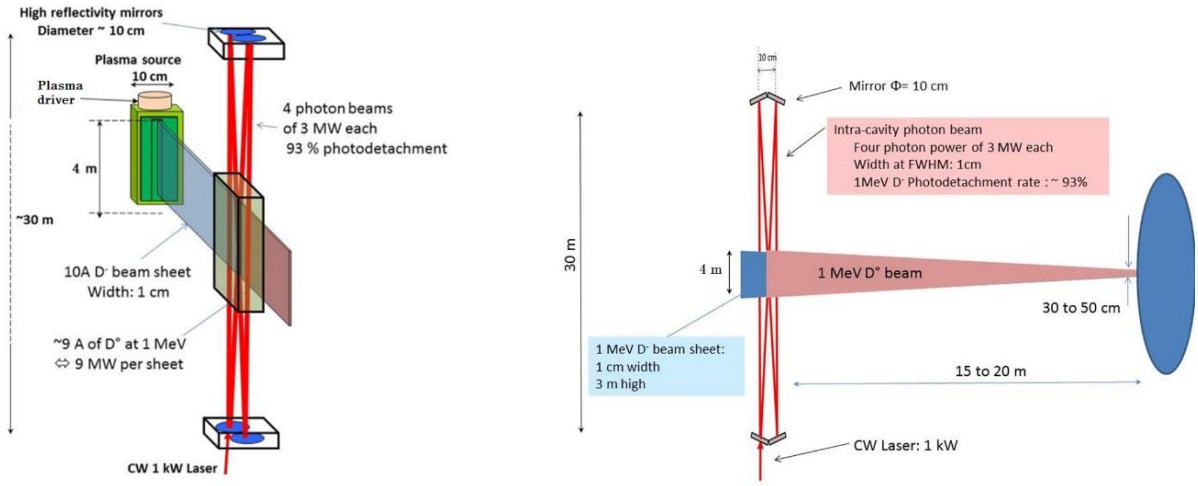

(a) (b)

FIGURE 1. (a) Schematic view of the photo-neutralization based system (b) *Topology of one cavity; it is a cavity composed with four mirrors (mirror diameter: 10 cm) aligned in the plane parallel to the ion beam; the single D^- ion beam sheet (4 m high) is crossed from top to bottom by four 3MW intra-cavity photon beam, leading to an overall neutralization rate of 93%.*;

Figure 1 shows the principle of a photoneutralization based injector, where an energetic 1 MeV blade-like negative ion beam of 4 m high and 1 cm width is crossed by vertical photon beams. The low photodetachment cross-section ($\sigma \approx 4.5 \cdot 10^{-21}$ m^2) [4] of the D^- ions requires powerful photon beam, indeed, 50% of neutralization rate for a 1 MeV D^- beam sheet over 1 cm width requires a 3 MW photon beam of 1 cm diameter at full width half maximum.

Such 3 MW photon power would be provided within a Fabry-Perot cavity composed of four high reflectivity mirrors (see Fig. 1-b) [5]. They are aligned in the plane parallel to the ion beam sheet, the cavity roundtrip is ~120 m long. With this cavity design, the blade-like ion beam is then fully crossed by four photon beams of 3 MW each (Fig 3a) leading to around 93% of neutralization rate.

Figure 2 shows the principle of a beamline (top view): it is composed of an ion source which produces the 10 A D^- blade-like beam which is pre-accelerated up to 100keV and then post-accelerated to 1 MeV in a single gap; the ion source is referenced to the ground potential and the neutralizer cell is held at 1 MV. The non-neutralized fraction of D^- (~ 1A) is decelerated down to 50 keV and collected on the recovery electrode. A calorimeter allows characterizing the ion beam optics before the injection into the tokamak plasma. Taking into account of the beam transmission and re-ionization in the duct, the neutral beam power injected within the plasma core would range around 8 MW per beam sheet.

It is important to point out that at full energy and neutral power, the power density on the calorimeter surface would exceed ~200 MW/m^2 (E=1MeV, I~8-9A, S_{beam}=4m*1cm) such thermal load cannot be sustained by any known existent materials. To diagnose the beam optics on the calorimeter at reduced power density (< 15 MW/m^2) , the photoneutralizer will operate at a low photoneutralization rate (less than 5% photodetachment), while the energy recovery system will collect the remaining 95% fraction of the negative ion beam current decelerated at a low energy (~9.5 A D^- per sheet at 50 keV). This new injector concept, called "SIPHORE" stands for **SI**ngle gap accelerator with **PHO**toneutralization and energy **RE**covery system.

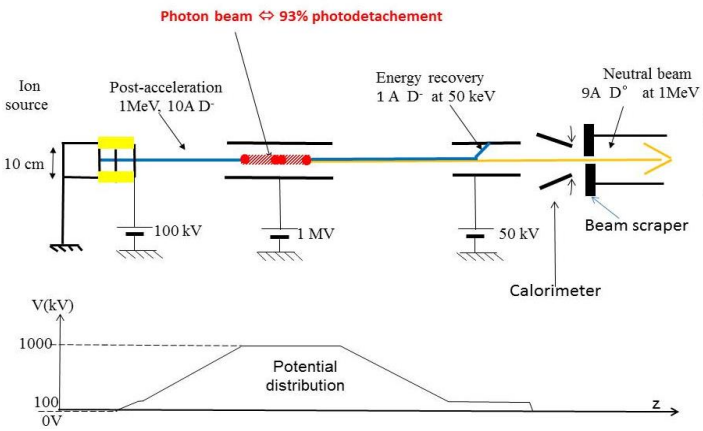

FIGURE 2. Schematic view of the negative ion beam acceleration, its neutralization, energy recovery system and potential distribution along the beamline.

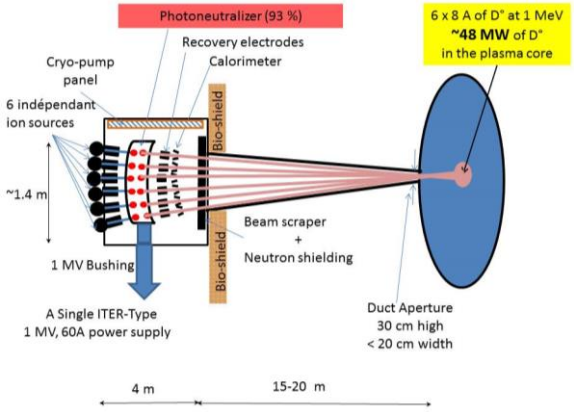

FIGURE 3. (a) *Top view of the SIPHORE injector based on six beams.*

A complete SIPHORE beamline powered by a single ITER-like 1 MV 60 A power supply is shown on Fig 3a: it is composed of six independent beam sheets implanted side by side and spatially oriented to focalize the six neutral beams within the Tokamak aperture, while the ion source and pre-accelerator are shaped to provide a vertical geometrical focalization of the neutral beam in the Tokamak port. The total neutral power coupled within the plasma core would range around ~48 MW. The photoneutralizer cell is sustained under vacuum and held at 1 MV by a 1 MV bushing implanted on one side of the photoneutralizer.

The tall and narrow injector aspect ratio (4 m height and 10 cm large) forces for development of a new type of ion source and accelerator to provide the 10 A of D^- beam sheet at the relevant D^- current density (J_{D^-} ~250 A/m^2) extracted from the plasma source.

ION SOURCE DEVELOPMENT FOR SIPHORE

Past experiments on Cybele

Cybele is a linear magnetized plasma source at IRFM (Fig.4a), used for the production of negative ion beams. The source dimensions (1.2m height, 15 cm width and 20 cm depth) are specifically adapted for the development of a D^- ion beam sheet. For this purpose, the source has to provide a hot and dense plasma (T_e >10 eV, $n_e > 10^{18}$ m^{-3}) in the center (see Fig. 4b) uniformly distributed along its vertical axis to induce a high level of molecular dissociation. In the extraction region (plasma edge) which is in contact with the accelerator grid (Fig. 4c), the plasma electrons are thermalized (T_e < 2 eV), and the negative ions will be produced by electron capture of the D° atoms bombarding the cesiated accelerator's metal surface.

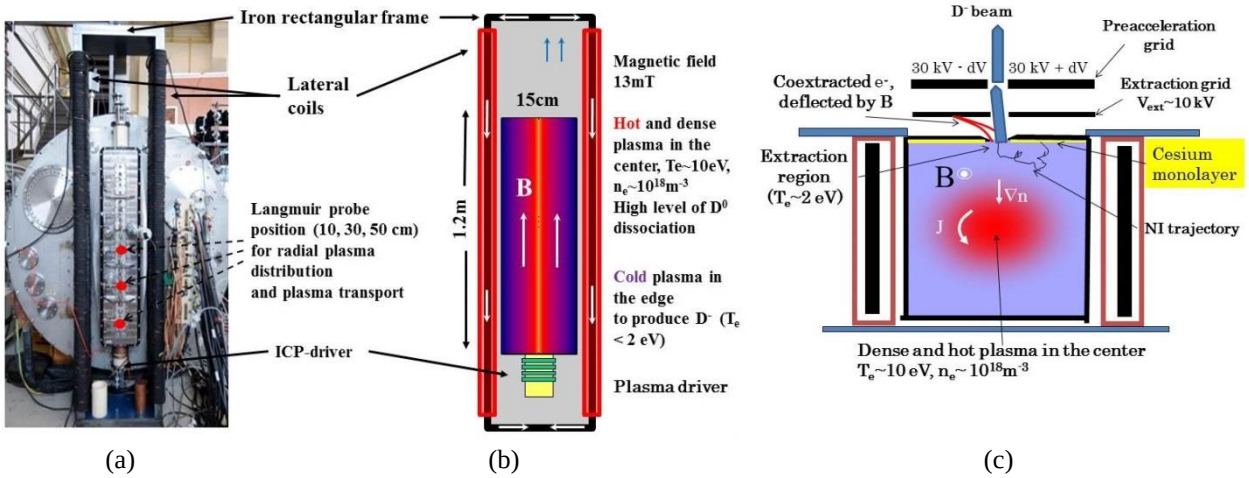

FIGURE 4. (a) The photo of Cybele ion source (front view) (b) Schematic view of Cybele (c) Schematic view of Cybele with beam extraction (top view).

In the preliminary experiments, Cybele was tested with a transverse magnetic filter (of 400 Gauss*cm) on the source front like conventional negative ion sources (ITER-type). It was observed a strong plasma inhomogeneity along the source vertical axis between the top and the bottom due to a diamagnetic plasma drift with an ion density at the top of the source 7 times higher than at the bottom [6].

To overcome this vertical plasma drift, another magnetic field configuration was investigated, where the magnetic field is parallel to the source vertical axis. The vertical magnetic field is created by the leakage (external) magnetic field of two lateral electric coils sitting on both sides of the source; the coils are set around an iron rectangular core (fig 4a and 4b) to enhance the field intensity in the source volume up to 13 mT.

The negative ions will be mainly produced on the accelerator's metal surface by the D° bombardment. To enhance the NI production, i.e., the electron capture by the atom, a cesium layer can be deposited on the surface (see Fig. 4c). In the extraction region, the plasma has to be cold ($T_e < 2$ eV) to avoid destruction of the D^- by collisions with hot electrons (the electron affinity level of the D^- atom is only 0.75 eV). The Extraction grid (EG) provides voltage (~10kV) to extract ions from the source. The co-extracted electrons will be deflected by the vertical magnetic field (B~10 mT) which diffuses from the source and they will be collected on EG surface. The Pre-acceleration grid (PG) accelerates the beam up to 30keV, and, to compensate the negative ion deflection by the magnetic field, a polarization ($\pm\delta V$) is applied between the two lateral plates of the grid to generate a transverse electric field.

This magnetic configuration (the magnetized plasma column) as shown in fig. 4b was tested first with filamented cathodes supplying the plasma centre with primary 70 eV electrons [3]. It was observed that the plasma was uniform along the source vertical axis due to the high electron mobility along the B-lines, with a rapid density drop at the two extremities due to the open magnetic field lines [3]. On the horizontal plane, as expected, the plasma density and temperature peaks in the center ($n_e = 5*10^{17}m^{-3}$ $T_e = 9$ eV for 30 kW of electrical power on the filamented cathodes) with a radial cooling towards the edges ($n_e \sim 1*10^{17}m^{-3}$ T_e~1-2eV) [3].

Present experimental set-up.

The filamented cathodes are undesirable in a future fusion reactor due to the limited lifetime and the plasma pollution by the evaporated tungsten, the second phase of the source development was devoted to the development of a radio-frequency plasma driver.

An Inductively Coupled Plasma (ICP) driver (f=1MHz) was installed on Cybele. The ICP driver is set in the bottom extremity of the Cybele source (Fig.4a) to inject the plasma particles in the direction parallel to the magnetic field in the Cybele chamber (column). It consists of a ceramic tube (inner diameter of 10 cm) with the helical antenna winded (9 windings, L ~11,5 mH) and a gas injection.

The electrical set up is shown on fig.5a: A DC breaker (RF transformer) was installed between the RF generator and the matching impedance box to decouple the two grounds (ground of the power supply and ground of the

source). It is a 1:3 RF transformer where the primary and secondary windings are sleeved with ferrite coils specially adapted for the 1 MHz frequency.

The generator has to be loaded on 50 Ohms impedance, the plasma resistance is expected to be around 2 Ω [12], and the matching impedance is performed by parallel (C1) and series capacitances (C2); a series capacitance can be tune from 0 to 2 nF (see fig.5a).

The system of gas injection consists of the set of two gas valves. The first one is for the gas puff essential to ignite the plasma (pressure 1.5Pa) and the second one allows keeping the gas pressure constant during the plasma discharge (p~0.3 Pa).

Langmuir probes were installed at three positions (10, 30 and 50 cm up from the exit of ICP-driver, see fig 4a) in the backside of the plasma source to measure the plasma axial distribution. The probes are movable to scan the plasma profile from the centre up to the chamber walls. In the exit of the probe's measuring circuit the low pass filter was applied in order to remove the 1 MHz RF noise.

In the top of the source is installed the camera for observing and recording the visible light coming from plasma, generated in the bottom part by ICP driver.

The vacuum tank is equipped with a turbomolecular pump and a cryopump (pumping speed 10^4 l/s). A typical discharge lasts around 5 s and the shots have a relatively high repetition rate (20 - 25 pulses per hour).

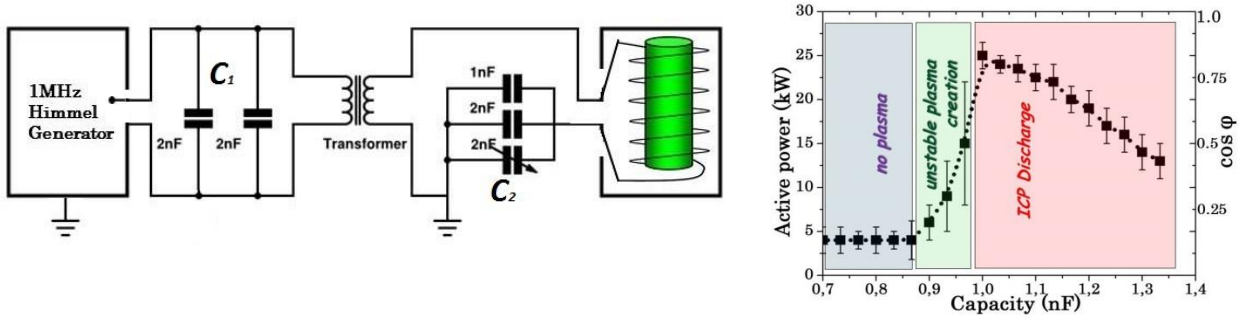

(a) (b)

FIGURE 5. (a) Schematic view of the electrical circuit of Cybele's ICP driver (b) The optimal value of power transferred to plasma is obtained from generator by changing the value of series capacitor.

EXPERIMENTAL RESULTS AND DATA ANALYSIS

Defining the matching

The first step of the experiments was to find the proper matching between the generator and the ICP-driver in order to couple a maximum of RF active power to the plasma.

The Fig.6b represents the value of $\cos\varphi=P_{act}/P_{app}$ (active and apparent power) and the P_{act} as a function of the C2 capacitance. The active power were defined as $P_{act}=P_{app}-P_{ref}$. Reflected (P_{ref}) and apparent (P_{app}) power are measured directly by 1MHz Himmel generator. Here three regimes were observed. The first one at low capacitance (C2 < 0.9 pF), the active power and cosφ are low (P_{act}~4 kW, cosφ≈0.12), the plasma is created by the capacitive coupling of the antenna. Between 0.9-1nF, the active power and cosφ rapidly increase but the plasma is unstable, the electrical measurements highlight strong RF oscillations.

The peak (C2=1 pF) corresponds to the best matching: the plasma is stable, the cosφ ranges around 0.75-0.8 (low reflected power). Under this configuration, the change or scan of the plasma parameters (RF power, source operating pressure, magnetic field) do not significantly affect the matching; only a slight modification of the C2 capacitance is necessary to get back to the optimum.

Plasma parameters

The plasma parameters (n_e, T_e, V_{pl}, V_{float}) were measured by the Langmuir probe which is biased by a pulsed generator to provide a sequence of ramps (voltage sweep ±60V) with a period of 60 ms during the plasma discharge; the averaging over 20 ramps allows to minimize the error-bars of the probe characteristics (I_{probe} vs. V_{probe}).

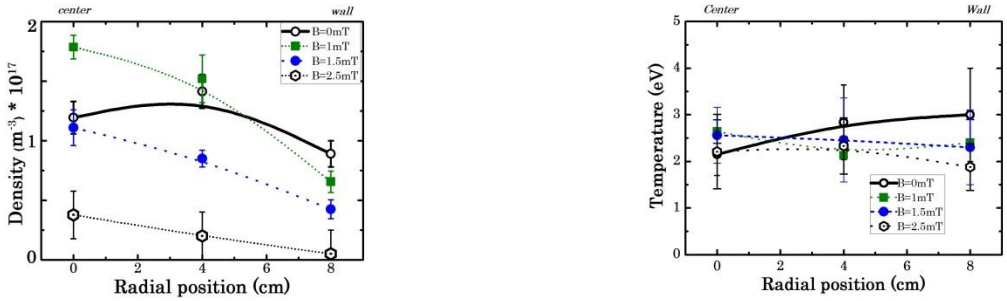

(a) (b)

FIGURE 6. (a) Radial distribution of plasma density (b) Radial distribution of plasma temperature. (Different lines indicate different values of external magnetic field, power 30kW, pressure 0.3Pa, Hydrogen, 10cm from driver exit)

Fig.6 represents the radial profiles of plasma density and temperature with 30 kW of active RF power for different magnetic field intensities; the probe is positioned at 10 cm above the driver exit. Without external magnetic field (B=0), the plasma density is nearly flat (black solid line). With increasing of magnetic field plasma density is approximately twice higher in the center compare to the edges. The electron temperature is almost constant between the center and edges for all values of external magnetic field and ranges between 1.5 and 4 eV. It is the characteristic of a typical plasma which expands under an ambipolar diffusion in the direction parallel to B: the electrons are thermalized by collisions in the ICP driver, and the diffusion inside NI source volume results from plasma particle collisions effect. The plasma density is relatively low: the maximum density obtained is only 1.7 $10^{17}m^{-3}$ for 30 kW of RF power, 1mT magnetic field at 10 cm from driver exit.

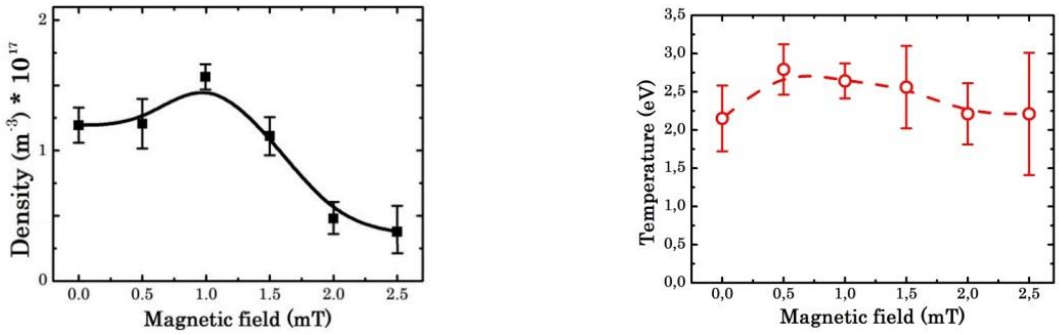

(a) (b)

FIGURE 7. (a) Plasma density as a function of external axial magnetic field (b) Plasma temperature as a function of external axial magnetic field (10 cm from driver exit, 0.3 Pa pressure, 30 kW of power injected to plasma, Hydrogen).

The variation of the density and temperature as function of magnetic field for 30 kW of active RF power is presented on fig.7; the probe is set up at 10 cm above the plasma driver exit. Without magnetic field, the density ranges around $1.2*10^{17}$ m^{-3}, and peaks to $1.7*10^{17}$ m^{-3} with 1 mT magnetic field. Above 1 mT, the plasma density rapidly decreases and after 2.5 mT plasma generation stops (plasma cut-off).

The effect of the external vertical magnetic field on the inductively coupled plasma generation is likely due to the increase of the plasma resistivity in the plane perpendicular to the magnetic field. The azimuthal inductive electron current which flows in the plane perpendicular to B, experiences a Lorentz force ($\mathbf{v_e x B}$, where $\mathbf{v_e}$ is the

electron velocity and **B** is the external (vertical) magnetic field), which reduces the electron mobility: the transverse plasma conductivity ($\Gamma_\perp$) is 60 times lower than the parallel conductivity ($\Gamma_{//}$) :

$$\Gamma_\perp = \frac{(\nu_c - i\omega)\omega_{ce}}{(\nu_c - i\omega)^2 + \omega_{ce}^2} \cdot \Gamma_{//} \sim \frac{1}{60} \cdot \Gamma_{//}$$

where ν_c is the electron collision frequency (~10^7 s^{-1}) and ω_{ce} is the electron cyclotron frequency (~ $6*10^8$ s^{-1} at 3 mT)[7]. So, in this configuration electrons are more magnetized, their Larmor radius becomes smaller with applying of external vertical magnetic field and less ionization collisions with the neutral atoms occur in the direction perpendicular to the B-field. Finally, with increasing of the vertical magnetic field intensity the azimuthal current, produced by an ICP-antenna, decreases, what is leading to the drop of plasma density. In some extreme values of magnetic fields (for us it is 2.5mT), the amount of electrons inside the driver is insufficient to keep plasma ionized which causes the plasma cut-off.

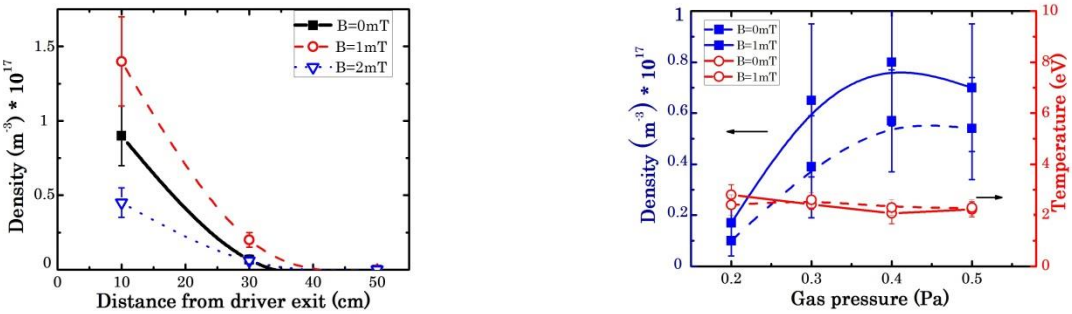

(a) (b)

FIGURE 10. (a) Plasma density distribution along the vertical axis with different values of magnetic field (0.3 Pa pressure, 30 kW of power injected to plasma, Hydrogen) (b) Plasma density (blue squares) and plasma temperature (red circles) as a function of gas pressure with (solid line) and without (dashed line) magnetic field. (10 cm from driver exit, 30 kW of power injected to plasma, Hydrogen)

The plasma transport (diffusion) in the NI source for different intensities of magnetic field is illustrated in fig.10a. Without magnetic field, we can observe that the plasma density is rapidly decreasing along the NI source axis: the density drops between 10 cm and 30 cm away from the driver exit is important, and, at mid-height of the NI source (50 cm away from the driver), the plasma density is below the probe resolution (less than 0.5 $10^{16}m^{-3}$). At B=1 mT, we note a higher density in the source volume, so B-filed pushes plasma toward the center of plasma source, but the rate of plasma density decay is the same as without magnetic field (7 times less plasma density at 30 cm from driver exit compare to the 10 cm).

The effect of the gas pressure on the plasma density (blue squares) and temperature (red circles) is shown in fig.10b. We observe a linear increase of the density with the pressure between 0.2 to 0.4 Pa with a saturation above. It was impossible to ignite the plasma at a pressure lower than 0.2 Pa. The electron temperature is slightly decreasing from 3 to 2.2 eV with the plasma collisionality (the pressure increase).

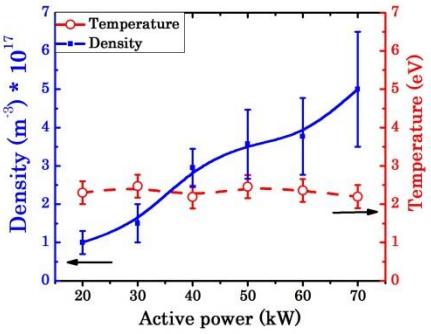

(a)

FIGURE 11. (a) Plasma density and plasma temperature as a function of the active power (10 cm from ICP driver exit, 0.3 Pa pressure, Hydrogen, without magnetic filed).

The fig.11 shows the plasma density (blue squares) and temperature (red circles) as the function of active power transferred to plasma magnetic fields B=1mT. The density is linearly increasing with increasing the active power. The electron temperature is measured between 2 and 2.7 eV for all the values of input power.

The table 1 below compares the plasma density (n_e) and electron temperature (T_e) obtained on Cybele equipped with the heated cathodes (filaments) and with the ICP-driver for the same input power (30 kW) with 0.3 Pa in Hydrogen; the table shows that the ICP driver is less efficient to provide a hot and dense plasma in the source center.

Table 1

Power= 30 kW	n * 10^{17}(m^{-3})	T_e (eV)	
		center	edge
Filaments	5	9	2
ICP	1.7	2.5	~2.5

HELICON PLASMA SOURCE DEVELOPMENT

In 2012 IRFM CEA Cadarache started collaboration with EPFL for the development of the Helicon plasma driver dedicated to the Cybele ion source (B~10 mT, operating pressure lower than 0.3 Pa).

For this purpose, a bird-cage type helicon antenna of 10 kW has been designed and tested on the RAID testbed at EPFL [8-10].

Recent investigations in RAID testbed of the negative ion production showed quite promising results[11]:

-i) the plasma produced by the Helicon driver has a desirable radial cooling, from 6eV in the center of plasma column down to 2eV on the edge;

-ii) the plasma density is relatively high in the center (n_e~8*$10^{17}m^{-3}$) with only 3-5 kW of RF power with an operating pressure of 0.3 Pa in Hydrogen;

-iii) a significant negative ion density was detected in the plasma edge; the H^- density is estimated to ~2.5*$10^{16}m^{-3}$.

The comparison of the Helicon antenna with the ICP driver performances reveals that the Helicon plasma driver seems to be the best candidate to provide a dense and uniform magnetized plasma column on the Cybele source.

Finally, the new 10kW Helicon antenna was successfully installed and commissioned on Cybele in December 2016, it will be tested then in negative ion production in 2017.

CONCLUSIONS

The Cybele ion source with the vertical magnetic field topology has been tested with the ICP driver implanted at the bottom extremity of the source, to inject the plasma particles in the direction parallel to B.

It was observed a non-uniform plasma distribution along the source axis (rapid drop of plasma density) which results from an ambipolar plasma diffusion along B. The plasma profile (density and temperature) is flat, the density

is lower than with the filamented cathodes for the same input power and the electron temperature ranges around 1.5-3.5eV. It was also observed a strong limitation of the inductive coupling with external vertical magnetic field due to the increase of the plasma resistivity in the plane perpendicular to B; a plasma cut-off occurs for B higher than 2.5 mT.

Recent experiments on the RAID testbed (EPFL) highlighted that the Helicon antenna seems to be the best plasma driver for Cybele. This 10kW Helicon antenna was installed and commissioned on Cybele in December 2016, it will be tested then in negative ion production in 2017.

AKNOWLEDGEMENTS

This work benefited from financial support by the French National Research Agency (Agence Nationale de la Recherche; ANR) in the framework of the project ANR-13-BS04-0016 (Siphore), ANR-13-BS09-0017 (H-Index), by the PACA county in the framework of the project "dossier 2011_11042" (PACA Siphore) and "dossier 2012_10357" (PACA-Ging). This work has been carried out within the framework of the EUROfusion Consortium and has received funding from the Euratom research and training programme 2014-2018 under grant agreement No 633053. The views and opinions expressed herein do not necessarily reflect those of the European Commission.

REFERENCES

1 G. Giruzzi, et al., "Modelling of pulsed and steady-state DEMO scenarios", Nucl. Fusion 55 (2015) 073002 (14pp)
2 Franke T et al "On the present status of the EU DEMO H&CD systems, technology, functions and mix" Poster SP13-63 26th SOFE Conf. Proc. 2015 (Austin, Texas USA)
3 A. Simonin et al., "R&D around a photoneutralizer-based NBI system (Siphore) in view of a DEMO Tokamak steady state fusion reactor", Nucl. Fusion **55** (2015) 123020 (19pp).
4 Vandevraye M., Babilotte P., Drag C. and Blondel C. 2014 *Phys. Rev.* A **90** 013411.
5. W. Chaibi et al. "Photo-neutralization of Negative Ion Beam for future fusion reactor", Proceedings of the 1st International Symposium of Negative Ion Beams and Sources, NIBS Conference proceedings, Aix-en-Provence, France, September 2008.
6 A. Simonin, L. Christin, H.P.L. De-Esch, R. Futtersack, P. Garibaldi, F. Villecroze, "Mirror-like plasma confinement for a uniform large negative ion source", Nucl. Fusion 52 (2012) 063003 (7pp).
7 J.A. Bittencourt; Fundamental of plasma physics; Pergamon press, 1986.
8 Ph. Guittienne, E. Chevalier, Ch. Hollenstein, "Towards an optimal antenna for helicon waves excitation", 2005, Journal of Applied Physics 98, 083304.
9 Ch. Hollenstein, Ph Guittienne, A.A. Howling, 2013, Plasma Sources Sci. Technol. 22, 055021.
10. A A Howling, Ph Guittienne, R Jacquier and I Furno, "Complex image method for RF antenna-plasma inductive coupling calculation in planar geometry. Part I: basic concepts", Plasma Sources Sci. Technol. 24 (2015) 065014 (8pp).
11 C Marini, et al., "Spectroscopic characterisation of H2 and D2 helicon plasmas generated by a resonant antenna for neutral beam applications in fusion", submitted to Nuclear Fusion.
12. M.A. Liberman and A.J. Lichtenberg, Principles of Plasma Discharges and Material Processing, Sec.Ed., pp. 460-469, John Willey & Sons, Inc., 2005.